DISILICON CARBIDE (Si$_2$C) IN THE INTERSTELLAR MEDIUM

M.K.SHARMA[1], S.CHANDRA[2]

The Si$_2$C and SiC$_2$ both are considered to play key role in the formation of the SiC dust grains in the atmosphere of the carbon-rich stars. The molecule of our interest Si$_2$C has been detected in the envelope of the red supergiant star IRC+10216 first time. It is an asymmetric top molecule having electric dipole moment of 1 Debye along the *b*-axis of inertia. Because of zero nuclear spin of both the Carbon and Silicon atoms, it has only paratransitions. Using the given spectroscopic data (rotational and centrifugal distortion constants and electric dipole moment), for the para-Si$_2$C, we have calculated energies of 200 lower rotational levels (having energy up to 217.8 cm^{-1}) and the Einstein *A* and *B* coefficients for 867 radiative transitions between the levels. We have solved a set of 200 statistical equilibrium equations coupled with 867 equations of radiative transfer (Sobolev analysis), where the collisional rate coefficients are taken from a scaling law. Out of 867 radiative transitions, 13 transitions have been found showing weak MASER action, and 19 transitions showing anomalous absorption. One transition 8_{08}-7_{17} is found to show both the MASER action as well as the anomalous absorption. These transitions in addition to the observed transitions may play important role in the identification of Si$_2$C in the cosmic objects.

Keywords: *ISM:molecules - Si$_2$C - Sobolev LVG analysis - radiative transition*

1. *Introduction*. Out of a large number of molecules found in the interstellar medium (ISM), thirteen are bearing Si atom: SiO [1], SiH$_4$ [2], *c*-SiC$_2$ [3], SiS [4], SiC [5], C$_4$Si [6], SiN [7], *c*-SiC$_3$ [8], SiCN [9], SiNC [10], SiH$_3$CN [11], Si$_2$C [12], CH$_3$SiH$_3$ [13]. All the 13 have been detected in the envelope of red supergiant star IRC+10216. The SiO and SiS are also found in the massive-star forming regions, such as Ori KL and Sgr B2. Herbst et al. [14] carried out the detailed chemical model calculations for the Si-bearing molecules in the dense molecular clouds and estimated abundances of 23 Si-bearing molecules, and Si and Si$^+$. Five molecules, SiS, SiCN, Si$_2$C, SiH$_3$CN and CH$_3$SiH$_3$, which are not in the list of Herbst et al. [14], have also been identified in the IRC+10216.

Owing to zero nuclear spin for both the Carbon C and Silicon Si atoms, there are only para rotational levels in the ground vibrational state of Si$_2$C - the molecule of interest. Cernicharo et al. [12] have detected first time the Si$_2$C in the IRC+10216 through four transition, $3_{1.3}$-$2_{0.2}$, $16_{1.15}$-$16_{0.16}$, $18_{1.17}$-$18_{0.18}$ and 9_{28}-10_{19}. For the para-Si$_2$C, we have considered 200 lower rotational levels (having energy up to 217.8 cm^{-1}) connected through 867 radiative transitions. For the

kinetic temperature up to $100\,K$, considered here, the levels up to $217.8\,cm^{-1}$ are sufficient, and the contribution of further higher levels would not be significant. Besides the radiative transitions, the levels are connected through the collisional transitions as well. After solving a set of statistical equilibrium equations coupled with the equations of radiative transfer, we have found 13 transitions showing weak MASER action, and 19 transitions showing anomalous absorption. One transition 8_{08}-7_{17} is found to show both the MASER action and the anomalous absorption. These lines along with the observed transitions may play important role for identification of Si_2C in a cosmic object.

2. *The Si_2C molecule*. The disilicon carbide (Si_2C) is a planar, *b*-type asymmetric top molecule having C_{2v} symmetry and a $^1A_1$ electronic ground state. Its electric dipole moment 1 Debye lies along the *b*-axis of inertia [15-19]. High resolution spectrum of Si_2C is recorded by McCarthy et al. [19], and accurate rotational and centrifugal distortion constants derived by them in I^r Watson Hamiltonian with A-reduced representation are given in Table 1 (column 2), and with the S-reduced representation (column 3). As the constants in both the representations have been derived from the same spectrum, they would provide the similar results for the energies of rotational levels, and the line-strengths. There is no preference for the use of the A-reduced representation data in the present investigation.

Using the rotational and centrifugal distortion constants (column 2), we have calculated energies of 200 lower rotational levels of para-Si_2C with the help of

Table 1

ROTATIONAL AND CENTRIFUGAL DISTORTION CONSTANTS
IN MHz OF Si_2C

Constant	A-reduction	S-reduction
A	64074.33623 (37)	64074.3366 (44)
B	4395.621072 (844)	4395.51772 (41)
C	4102.02789 (107)	4102.13098 (62)
$D_J \cdot 10^3$	9.73150 (178)	9.66776 (224)
D_{JK}	-0.8572075 (610)	-0.856833 (73)
D_K	23.58805 (148)	23.58788 (178)
$d_J \cdot 10^3$	1.519832 (437)	-1.52630 (34)
$d_K \cdot 10^2$	5.1591 (454)	-0.00318 (32)
$H_J \cdot 10^8$	-4.1349 (949)	-3.627 (116)
$H_{JK} \cdot 10^5$	1.93298 (547)	1.9373 (67)
$H_{KJ} \cdot 10^3$	-1.88755 (791)	-1.8882 (95)
$H_K \cdot 10^2$	4.8633 (168)	4.8632 (204)
$h_J \cdot 10^9$	-5.231 (187)	-5.304 (225)
$h_{JK} \cdot 10^9$	-6586 (361)	-2.614 (255)

the software ASROT [20]. Rotational levels are denoted by $J_{k_a k_c}$, where J stands for the rotational quantum number, and the k_a and k_c are the projections of J on the axis of symmetry in case of prolate and oblate symmetric tops, respectively. As the nuclear spin of both the Si and C atoms is zero, we have only the transitions between the levels with $k_a + k_c = $ even integer.

3. *Model*. As the kinetic temperature in the regions where Si$_2$C may be found is very low (few tens of Kelvin), we are concerned with the rotational levels in the ground vibrational state and ground electronic state. The energy levels are connected through the radiative transitions and the transitions due to collisions with the most abundant molecule, hydrogen molecule H$_2$. We have considered 200 lower rotational levels and expressed the statistical equilibrium equations coupled with the equations of radiative transfer as the following [21]:

$$n_i \sum_{\substack{j=1 \\ j \neq i}}^{200} P_{ij} = \sum_{\substack{j=1 \\ j \neq i}}^{200} n_j P_{ji} \qquad i = 1, 2, ..., 200 \tag{1}$$

where n are the population-densities of levels and the parameters P are expressed as the following:

(i) For radiative transitions

$$P_{ij} = \begin{cases} \left(A_{ij} + B_{ij} I_{v,bg}\right)\beta_{ij} + n_{H_2} C_{ij} & i > j \\ B_{ij} I_{v,bg}\, \beta_{ij} + n_{H_2} C_{ij} & i < j. \end{cases} \tag{2}$$

(ii) For collisional transitions

$$P_{ij} = n_{H_2} C_{ij}, \tag{3}$$

where $I_{v,bg}$ is the intensity of cosmic background radiation, A and B are the Einstein coefficients for radiative transitions, and C - the collisional rate coefficients. The n_{H_2} is the density of molecular hydrogen in the region, and the escape probability β for the transition between upper level u and lower level l is

$$\beta_{lu} = \beta_{ul} = \frac{1 - \exp(-\tau_v)}{\tau_v}, \tag{4}$$

where the optical thickness τ_v for the radiation is

$$\tau_v = \frac{hc}{4\pi(d v_r/dr)}\left[B_{lu} n_l - B_{ul} n_u\right] \tag{5}$$

where $d v_r/dr$ is the velocity-gradient in the region. Here, the external radiation field, impinging on a volume element generating the lines, is the cosmic microwave background (CMB) only with the background temperature $T_{bg} = 2.73$ K. Equation (1) is a set of homogeneous equations, which cannot have a unique solution. In order to make the set of equations inhomogeneous to have a unique solution, one of the statistical equilibrium equations is replaced by the following equation.

$$\sum_{i=1}^{200} n_i = n_{mol} \; . \tag{6}$$

where n_{mol} is the total density of Si_2C molecule in the region. The required input parameters for solving this set of equations are the radiative transition probabilities (Einstein A and B coefficients) and the collisional rate coefficients for the transitions between the levels.

3.1. *Radiative transition probabilities*. The Si_2C is *b*-type asymmetric top molecule where radiative transitions are governed by the selection rules:

$$J: \quad \Delta J = 0, \pm 1$$
$$k_a, k_c: \quad \text{even, even} \leftrightarrow \text{odd, odd} \quad (\text{para - transition}).$$

Using the rotational and centrifugal distortion constants (Table 1 column 2) and the electric dipole moment, we have calculated line strengths S_{ul} of transitions with the help of the software ASROT [20]. For a transition from upper level u to lower level l, the line-strength $S_{ul} (= S_{lu})$ is related to the Einstein A_{ul}-coefficient through the relation

$$A_{ul} = \left(\frac{1}{2J_u + 1} \right) \frac{64\pi^4 \nu^3 \mu^2}{3hc^3} S_{ul} \, ,$$

where μ is the electric dipole moment and ν the frequency of transition. Among 200 levels, there are 867 radiative transitions. The Einstein A and B coefficients are related as:

$$A_{ul} = \frac{8\pi h \nu^3}{c^3} B_{ul} \quad g_u B_{ul} = g_l B_{lu} \, ,$$

where g_u and g_l are the statistical weights of upper and lower levels, respectively. These Einstein A and B coefficients are input data for solving the statistical equilibrium equations coupled with the equations of radiative transfer.

3.1.1. *Radiative life-time*. The radiative life-time T_j of a level j is defined as

$$T_j = 1 \Big/ \sum_i A_{ji} \, ,$$

where A_{ji} is the Einstein A-coefficient for a radiative transition from upper level j to lower level i, and the summation is taken for all the downward radiative transitions from the level j. In general, radiative life-time of upper level is smaller than that of the lower level. In case of the stimulated emission, the reverse is true and the excitation temperature for the transition is negative (population inversion).

3.2. *Collisional rates*. Though the collisional transitions do not follow any selection rules, but, their computation is difficult task [22-24]. However, one has to calculate the collisional rate coefficients for one direction (excitation or

deexcitation) of the transitions as for the transitions in the reverse direction can be calculated with the help of the detailed equilibrium [25]

$$C\left(J_{k_a,k_c} \to J'_{k'_a,k'_c}\right) = \left[\frac{2J'+1}{2J+1}\right] \exp\left[-\frac{\Delta E}{kT}\right] C\left(J'_{k'_a,k'_c} \to J_{k_a,k_c}\right),$$

where, ΔE is the magnitude of energy difference between the levels J_{k_a,k_c} and $J'_{k'_a,k'_c}$. The required collisional rate coefficients are not available in literature. When the collisional rate coefficients are not available in literature, various scaling laws have been used. In the present investigation, the deexcitation rate coefficients at kinetic temperature T are calculated with the help of the expression [26,27]

$$C\left(J'_{k'_a,k'_c} \to J_{k_a,k_c}\right) = \frac{1 \cdot 10^{-11}}{2J'+1}\sqrt{T}.$$

It is just the cross-section times the relative velocity of collision partner, which is the most abundant H$_2$ molecule in a molecular region.

4. *Results and discussion*. The non-linear set of statistical equilibrium equations coupled with the equations of radiative transfer is solved through the iterative method, where radiative and collisional transition probabilities are the input parameters. The initial population densities of levels are taken as the thermal ones. For inclusion of various types of cosmic objects, where the Si$_2$C may be found, wide ranges of physical parameters are considered. The molecular hydrogen density n_{H_2} is taken from 10^2 to $10^6\,\text{cm}^{-3}$; the kinetic temperatures T are 20, 40,

Table 2

FREQUENCY ν, EINSTEIN A-COEFFICIENT A_{ul}, ENERGY E_u
OF UPPER LEVEL, RADIATIVE LIFE-TIME t_u OF UPPER LEVEL
AND t_l OF LOWER LEVEL FOR 13 WEAK MASER TRANSITIONS
BETWEEN THE LEVELS OF Si$_2$C

Transition	ν (MHz)	A_{ul} (s^{-1})	E_u (cm^{-1})	t_u (s)	t_l (s)
$8_{0.8}$–$7_{1.7}$	12018.353	4.389E-09	10.188	2.28E+08	2.07E+05
$20_{1.19}$–$19_{2.18}$	19095.478	9.867E-09	62.382	2.55E+05	1.24E+04
$10_{0.10}$–$9_{1.9}$	31198.760	8.182E-08	15.557	1.22E+07	1.44E+05
$22_{1.21}$–$21_{2.20}$	41506.466	1.061E-07	74.714	2.05E+05	1.12E+04
$12_{0.12}$–$11_{1.11}$	50756.482	3.717E-07	22.050	2.69E+06	1.05E+05
$24_{1.23}$–$23_{2.22}$	64274.818	4.120E-07	88.179	1.60E+05	1.01E+04
$14_{0.14}$–$13_{1.13}$	70615.021	1.051E-06	29.663	9.51E+05	7.82E+04
$18_{1.17}$–$18_{0.18}$	88715.414	3.245E-06	51.188	3.08E+05	2.25E+05
$16_{0.16}$–$15_{1.15}$	90689.359	2.330E-06	38.392	4.29E+05	5.99E+04
$18_{0.18}$–$17_{1.17}$	110889.131	4.450E-06	48.231	2.25E+05	4.68E+04
$24_{1.23}$–$24_{0.24}$	114375.156	5.825E-06	88.179	1.60E+05	5.40E+04
$20_{0.20}$–$19_{1.19}$	131122.679	7.675E-06	59.176	1.30E+05	3.71E+04
$22_{0.22}$–$21_{1.21}$	151301.687	1.228E-05	71.223	8.14E+04	2.98E+04

60, 80 and 100 K. Two values of $\gamma = n_{mol}/(d\,v_r/dr)$ are taken as 10^{-5} and 10^{-6} cm^{-3} (km/s)$^{-1}$ pc.
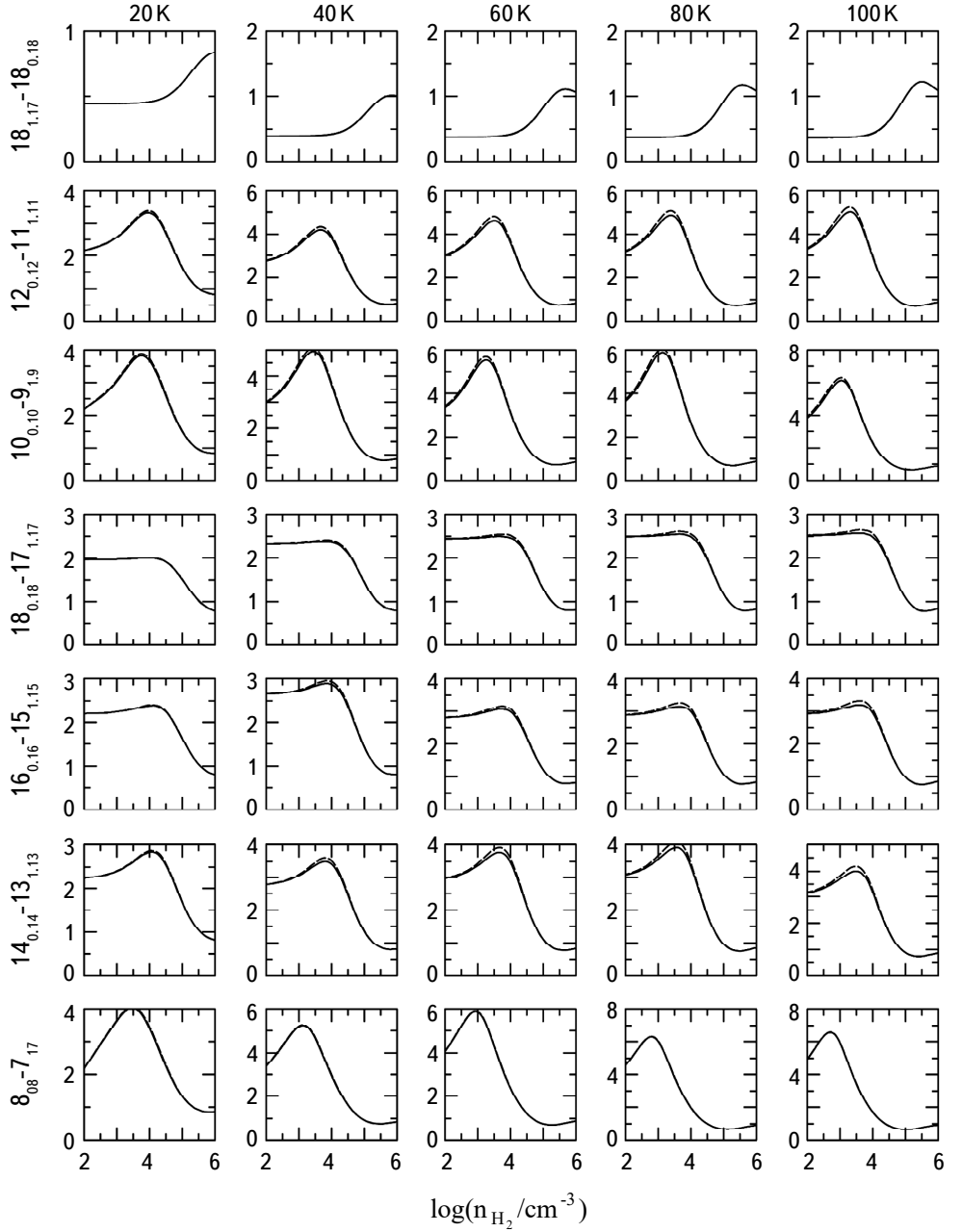

Fig.1. Variation of $n_u g_l/n_l g_u$ versus hydrogen density n_{H_2} for five kinetic temperatures T, written on the top, for seven MASER transitions, written on the left, of Si$_2$C molecule. Solid line is for $\gamma = 10^{-5}$ cm^{-3} (km/s)$^{-1}$ pc, and the dotted line for $\gamma = 10^{-6}$ cm^{-3} (km/s)$^{-1}$ pc.

For a MASER transition, the radiative life-time of upper level t_u is larger than that of the lower one t_l. However, larger life-time of upper level is not a sufficient criterion for the MASER action. For the MASER action, population inversion ($n_u g_l / n_l g_u > 1$) between the upper level u and the lower level l is also required. Here, n denotes the population density of level. For a radiative transition to be a weak MASER, two criteria are considered:

$$\frac{t_u}{t_l} > 1 \quad \text{and} \quad \frac{n_u g_l}{n_l g_u} > 1.$$

In the present investigation, we have taken $(t_u/t_l) > 1.2$ and $(n_u g_l / n_l g_u) > 1.2$. Out of 867 transitions, we have found 13 weak MASER lines. Information about these MASER transitions is given in Table 2, where we have given the frequency and Einstein A-coefficient of transition, energy of upper level, radiative life-times of upper and lower levels. For 7 MASER lines (written on the left) among the lowest levels, the variation of $n_u g_l / n_l g_u$ versus molecular hydrogen density n_{H_2} for kinetic temperatures of 20, 40, 60, 80 and 100 K, are given in Fig.1. The MASER action is in the region where $n_u g_l / n_l g_u$ is larger than 1. For these 7 lines, the MASER action is found to increase with the increase of kinetic temperature. At large densities, the MASER action may decrease or diminish as the collisions may destroy the population inversion.

At high densities, for a transition, both brightness temperature and excitation temperature tend to the kinetic temperature in the region (thermalization), whereas at low densities, the brightness temperature and excitation temperature both tend to the CMB temperature of 2.73 K. Meaning that the brightness temperature and excitation temperature of an spectral line should not be less than the CMB temperature of 2.73 K. But, 19 transitions of Si$_2$C have been found to show the excitation temperature less than 2 K (anomalous absorption). Information about the transitions is given in Table 3. The phenomenon of anomalous absorption has been observed for the transition 1_{10}-1_{11} of H$_2$CO [28] and the transition 2_{20}-2_{11} of c-C$_3$H$_2$ [29], for example.

For 7 anomalous absorption lines (written on the left) among the lower levels, the variation of excitation temperature T_{ex} versus molecular hydrogen density n_{H_2} for kinetic temperatures of 20, 40, 60, 80 and 100 K, are given in Fig.2. Anomalous absorption is in the region where the excitation temperature is less than 2.73 K.

The transition 8_{08}-7_{17} is found to show both the MASER action and the anomalous absorption. The MASER action of the transition 8_{08}-7_{17} is found at low density and low kinetic temperature. With the increase of the kinetic temperature, the MASER action is found to increase in the low density region and the anomalous absorption is found to appear and increase in the high density

Table 3

FREQUENCY ν, EINSTEIN A-COEFFICIENT A_{ul}, ENERGY E_u
OF UPPER LEVEL, RADIATIVE LIFE-TIME t_u OF UPPER LEVEL
AND t_l OF LOWER LEVEL FOR 19 ANOMALOUS ABSORPTION
LINES BETWEEN THE LEVELS OF Si_2C

Transition	ν (MHz)	A_{ul} (s^{-1})	E_u (cm^{-1})	t_u (s)	t_l (s)
$8_{0.8}-7_{1.7}$	12018.353	4.389E-09	10.188	2.28E+08	2.07E+05
$17_{2.16}-18_{1.17}$	2919.886	3.557E-11	51.285	1.38E+04	3.08E+05
$5_{1.5}-6_{0.6}$	6718.994	8.300E-10	6.169	3.12E+05	∞
$15_{2.14}-16_{1.15}$	24506.480	2.014E-08	41.950	1.53E+04	3.68E+05
$3_{1.3}-4_{0.4}$	24959.692	3.950E-08	3.664	4.89E+05	∞
$22_{2.20}-23_{1.23}$	37374.138	3.851E-08	79.900	1.21E+04	2.42E+04
$1_{1.1}-2_{0.2}$	42663.088	1.518E-07	2.272	7.25E+05	∞
$20_{2.18}-21_{1.21}$	44048.092	6.913E-08	67.648	1.30E+04	2.98E+04
$13_{2.12}-14_{1.13}$	45635.835	1.241E-07	33.743	1.70E+04	4.35E+05
$18_{2.16}-19_{1.19}$	52122.353	1.239E-07	56.543	1.41E+04	3.71E+04
$16_{2.14}-17_{1.17}$	61491.040	2.167E-07	46.584	1.53E+04	4.68E+04
$11_{2.10}-12_{1.11}$	66283.688	3.602E-07	26.665	1.88E+04	5.05E+05
$14_{2.12}-15_{1.15}$	72042.558	3.655E-07	37.770	1.67E+04	5.99E+04
$12_{2.10}-13_{1.13}$	83665.399	5.894E-07	30.098	1.83E+04	7.82E+04
$9_{2.8}-10_{1.9}$	86429.537	7.468E-07	20.717	2.07E+04	5.76E+05
$10_{2.8}-11_{1.11}$	96253.332	9.040E-07	23.567	2.00E+04	1.05E+05
$7_{2.6}-8_{1.7}$	106056.211	1.257E-06	15.900	2.24E+04	6.44E+05
$8_{2.6}-9_{1.9}$	109709.654	1.308E-06	18.174	2.17E+04	1.44E+05
$5_{2.4}-6_{1.5}$	125149.505	1.767E-06	12.216	2.40E+04	7.05E+05

region. This transition may guide to decide about physical conditions (temperature and density) in the region.

The observed transition $9_{28}-10_{19}$ is found to show the anomalous absorption, which is found to increase in the density-region with the decrease of temperature. The life-time of each of the levels 0_{00}, 2_{02}, 4_{04} and 6_{06}, is infinite. These levels connected through radiative transition with the nearest higher level are supposed to show the absorption lines. The transitions $1_{11}-2_{02}$, $3_{13}-4_{04}$, $5_{15}-6_{06}$ have been found to show anomalous absorption (Fig.2). The transition $1_{11}-0_{00}$ is not found to show anomalous absorption, as the level 2_{02} exists between the levels 1_{11} and 0_{00}. Since the level 3_{13} is higher than the level 1_{11}, the observed transition $3_{13}-2_{02}$ is not supported in our calculations. The observed transitions $16_{1.15}-16_{0.16}$ and $18_{1.17}-18_{0.18}$ have been found to show neither MASER action nor anomalous absorption. The observed lines along with 20 additional lines may play important role in the detection of Si_2C in a cosmic object.
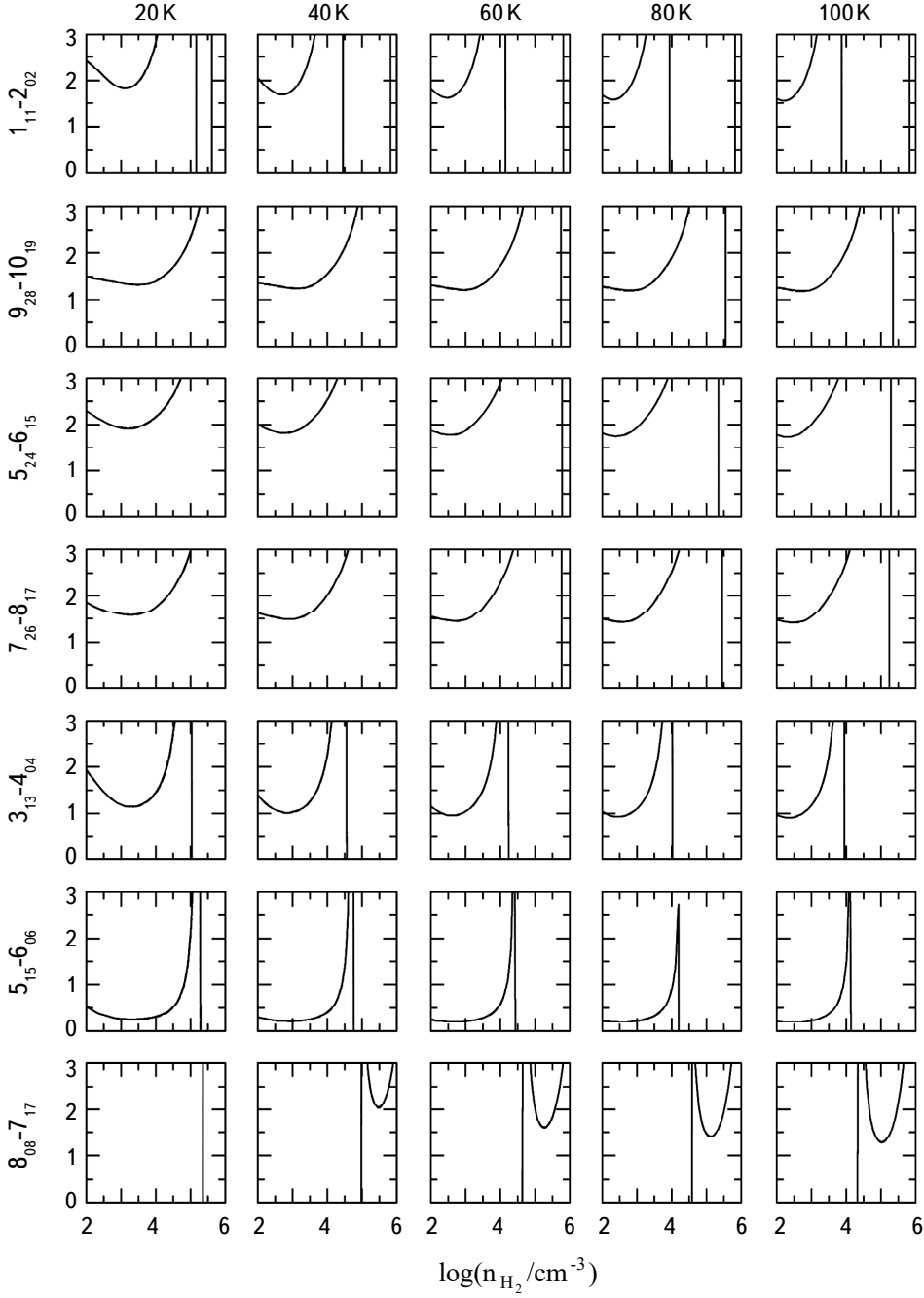
Fig.2. Variation of excitation temperature T_{ex} versus hydrogen density n_{H_2} for five kinetic temperatures T, written on the top, for seven anomalous absorption transitions, written on the left, of Si₂C molecule. Solid line is for $\gamma = 10^{-5}$ cm^{-3} (km/s)$^{-1}$ pc, and the dotted line for $\gamma = 10^{-6}$ cm^{-3} (km/s)$^{-1}$ pc.

5. *Conclusions*. After solving a set of 200 statistical equilibrium equations coupled with 867 radiative transfer equations of para Si_2C, we have found 13 weak MASER transitions and 19 anomalous absorption lines. Out of 4 observed lines, one transition 9_{28}-10_{19} has been found to show anomalous absorption. The observed transition 3_{13}-2_{02} is not supported in our calculations, as the level 1_{11} is lower than the level 3_{13}. Other two observed transitions $16_{1.15}$-$16_{0.16}$ and $18_{1.17}$-$18_{0.18}$ are found neither MASER lines nor anomalous absorption transitions.

[1] Physics Department, Sunder Deep Group of Institutions, NH-24, Delhi-Hapur Road, Dasna 201001, India, e-mail: mohitkumarsharma32@yahoo.in

[2] Amity Centre for Astronomy & Astrophysics, Amity Institute of Applied Sciences, Amity University, Sector 125, Noida 201313, U.P., India
e-mail: schandra2@amity.edu   suresh492000@yahoo.co.in

КАРБИД КРЕМНИЯ (Si$_2$C) В МЕЖЗВЕЗДНОЙ СРЕДЕ

М.К.ШАРМА[1], С.ЧАНДРА[2]

Принято считать, что Si_2C и SiC_2 играют ключевую роль в образовании пылинок SiC в атмосфере, богатых углеродом звезд. Молекула Si_2C впервые была обнаружена в оболочке красного сверхгиганта IRC+10216. Это молекула с асимметричным волчком, имеющая электрический дипольный момент 1 дебай вдоль оси инерции *b*. Из-за нулевого ядерного спина как атомов углерода, так и атомов кремния он имеет только парапереход. Используя приведенные спектроскопические данные (вращательные и центробежные константы дисторсии и электрический дипольный момент) для пара-Si_2C, рассчитаны энергии 200 нижних вращательных уровней (имеющих энергию до $217.8\,см^{-1}$) и коэффициенты Эйнштейна A и B для 867 радиационных переходов между уровнями. Решена система из 200 уравнений статистического равновесия в сочетании с 867 уравнениями переноса излучения (анализ Соболева), где коэффициенты частоты столкновений взяты из скейлингового закона. Из 867 радиационных переходов были обнаружены 3 перехода со слабым мазерным действием и 19 переходов с аномальным поглощением. Обнаружено, что один

переход 8_{08}-7_{17} демонстрирует как мазерное действие, так и аномальное поглощение. Эти переходы в дополнение к наблюдаемым переходам могут сыграть важную роль в идентификации Si$_2$C в космических объектах.

Ключевые слова: *ISM:молекулы - Si$_2$C - анализ Соболева LVG - радиационный переход*

REFERENCES

1. *L.E.Snyder*, *D.Buhl*, Astrophys. J., **189**, L31, 1974.
2. *D.M.Goldhaber*, *A.L.Betz*, Astrophys. J., **279**, L55, 1984.
3. *P.Thaddeus*, *S.E.Cummins*, *R.A.Linke*, Astrophys. J., **283**, L45, 1984.
4. *B.E.Turner*, Astron. Astrophys., **183**, L23, 1987.
5. *J.Cernicharo*, *C.A.Gottlieb*, *M.Guélin et al.*, Astrophys. J., **341**, L25, 1989.
6. *M.Ohishi*, *N.Kaifu*, *K.Kawaguchi et al.*, Astrophys. J., **345**, L83, 1989.
7. *B.E.Turner*, Astrophys. J., **45**, L35, 1992.
8. *A.J.Apponi*, *M.C.McCarthy*, *C.A.Gottlieb et al.*, Astrophys. J., **51**6, L103, 1999.
9. *M.Guélin*, *M.Müller*, *L.Cernicharo et al.*, Astron. Astrophys., **363**, L9, 2000.
10. *M.Guélin*, *M.Müller*, *L.Cernicharo et al.*, Astron. Astrophys., **426**, L49, 2004.
11. *M.Agundez*, *J.Cernicharo*, *M.Guélin*, Astron. Astrophys., A45, 570, 2014.
12. *J.Cernicharo*, *M.C.McCarthy*, *C.A.Gottlieb et al.*, Astrophys. J. Lett., **806**, L3, 2015.
13. *J.Cernicharo*, *M.Agundez*, *L.Velilla Prieto et al.*, Astron. Astrophys., **606**, L5, 2017.
14. *E.Herbst*, *T.J.Millar*, *S.Wlodak et al.*, Astron. Astrophys., **222**, 205, 1989.
15. *V.Barone*, *P.Jensen*, *C.Minichino*, J. Mol. Spectrosc., **154**, 252, 1992.
16. *E.E.Bolton*, *B.J.DeLeeuw*, *J.E.Fowler et al.*, J. Chem. Phys., **97**, 5586, 1992.
17. *W.Gabriel*, *G.Chambaud*, *P.Rosmus et al.*, Astrophys. J., **398**, 706, 1992.
18. *A.Spielfiedel*, *S.Carter*, *N.Feautrier et al.*, J. Phys. Chem., **100**, 10055, 1996.
19. *M.C.McCarthy*, *J.H.Baraban*, *P.B.Changala et al.*, J. Phys. Chem. Lett., **6**, 2107, 2015.
20. *Z.Kisiel*, *J.Demaison et al.*, Spectroscopy from Space. Kluwer, Dordrecht, 91, 2001.
21. *M.K.Sharma*, *M.Sharma*, *S.Chandra*, Astrophys. Space Sci., **362**, 168, 2017.
22. *M.Sharma*, *M.K.Sharma*, *U.P.Verma et al.*, Adv. Space Res., **54**, 252, 2014.
23. *M.K.Sharma*, *M.Sharma*, *U.P.Verma et al.*, Adv. Space Res., **54**, 1963, 2014.
24. *M.K.Sharma*, *S.Chandra*, Astrophys. Astron., **42**, 112, 2021.
25. *S.Chandra*, *W.H.Kegel*, Astron. Astrophys., **142**, 113, 2000.
26. *M.K.Sharma*, *S.Chandra*, Astrophysics, **64**, 388, 2021.
27. *M.K.Sharma*, *S.Chandra*, Astrophys. Astron., **42**, 112, 2021.
28. *P.Palmer*, *B.Zuckerman*, *D.Bhul et al.*, Astrophys. J., **156**, L147, 1969.
29. *S.C.Madden*, *W.M.Irvine*, *H.E.Matthews et al.*, Astron. J., **97**, 1403, 1989.